

# Physicochemical features of polyaniline supported heteropolyacids

A. POPA, NICOLETA PLEȘU, V. SASCA, E. E. KIȘ<sup>a</sup>, RADMILA MARINKOVIĆ-NEDUČIN<sup>a</sup>

*Institute of Chemistry of Romanian Academy Timișoara, Bl. Mihai Viteazul 24, Romania*

*<sup>a</sup>University of Novi Sad, Faculty of Technology, Cara Lazara 1, Novi Sad, Serbia and Montenegro*

Polyaniline with incorporated heteropolyanions was prepared by using a two-step reaction. This method involved synthesis of polyemeraldine base by polymerisation of aniline followed by deprotonation with ammonia. Then polyemeraldine base was protonated with heteropolyacid (HPAs) in a mixture water: ethanol = 1:1. The structure and texture of  $H_3PMo_{12}O_{40}$  (HPMo) and  $H_4PVMo_{11}O_{40}$  (HPVMo) supported on polyaniline was studied by XRD, FT-IR, low temperature nitrogen adsorption and scanning electron microscopy (SEM) with EDS analysis. Thermal stability of both HPAs supported on polyaniline was studied by TG and DSC measurements. The thermal decomposition of PANI support started at ca. 400°C, while for PANI-supported HPAs a decrease of decomposition temperature are observed. FT-IR studies showed that HPAs anions preserved their Keggin structure after deposition on polyaniline support. X-ray diffraction and SEM studies confirmed the uniformity of the distribution of active phase in the catalyst samples. The values of specific surface area of both HPAs increased by deposition on polyaniline support. It is found that most of HPMo and HPVMo (active phases) in samples are well dispersed on the support and polyaniline-supported HPA still keeps its Keggin structure. The surface morphology of the PANI-supported samples is almost similar to that of PANI support. A relatively uniform distribution of active phase in the support pores was evidenced by EDS analysis.

(Received May 25, 2006; accepted September 13, 2006)

**Keywords:** Heteropolyacids, Polyaniline, Texture, Structure, Thermal stability, BET, SEM, XRD

## 1. Introduction

Heteropolyacids (HPAs) with Keggin structure have been widely used in acid-catalysed reactions as well as oxidation reactions both in the heterogeneous and homogeneous systems [1-5]. Pure HPAs generally show low catalytic reactivity owing to their small surface area. In order to be more effective for catalytic reactions, HPAs are usually impregnated on different porous materials [6-14] and polymers [15-20].

Polymer materials have been widely used in chemical reactions as supports or catalysts due to their flexible applicability [15-22].

Polyaniline (PANI) is a conductive polymer, is cheap and stable to heat and air atmosphere. It is also the first commercially available conducting polymer. PANI refers to a class of polymers, which the polymeric chain consists of a succession of reduced benzenic nucleus and oxidised quinoidic nucleus.

The synthesis and the characterisation of PANI doped with different anions are critical since many properties of the final polymer are greatly influenced by the nature of the doping ion, properties that provide the special destination of it. The first attempt of the electrocatalytic application of PANI was mentioned by Keita et al [27] and Bidan et al [28] by incorporation of Keggin type heteropolyanions into PANI. M.Hasik et al [15, 16] show that PANI base can be used as convenient catalytic support on which non-oxidising heteropolyanions can be dispersed via protonation. This protonation reaction results in the formation of an ionic bond between heteropolyanions and the support and should also modify the acid-base properties of the catalyst.

HPAs catalysts immobilized on conjugated conducting polymers have found successful applications as heterogeneous catalysts in some vapor-phase reactions such as ethanol and 2-propanol conversion [15-17, 19]. The type of carrier, textural and structural properties influence the thermal stability and the catalytic activity of Keggin-type heteropolyacids.

In order to obtain highly dispersed heteropolyacids species,  $H_3PMo_{12}O_{40}$  and  $H_4PVMo_{11}O_{40}$  were supported on polyaniline (PANI). The goal of this work was to characterise the texture and structure of these heteropolyacids supported on polyaniline in reference to the bulk solid heteropolyacids.

## 2. Experimental

$H_4 [PMo_{11}VO_4] \cdot 12H_2O$  was prepared by two methods: Tsigdinos and hydrothermal method [29-30]. In both cases HPAs were crystallized slowly from aqueous solutions at room temperature.  $H_3[PMo_{12}O_{40}] \cdot 13H_2O$  was purchased from Merck. The as-received material was recrystallized prior to use. They are stable at room temperature with 12-14  $H_2O$  molecules.

Polyaniline (PANI) with incorporated heteropolyanions was prepared by using a two-step reaction. This method involved synthesis of polyemeraldine base by polymerization of aniline with  $(NH_4)_2S_2O_8$  in HCl followed by deprotonation with ammonia [15-18]. The HPA active phase deposition on the PANI support was performed by protonation from water : ethanol = 1:1 solution. The HPMo and HPVMo acids were deposited by protonation in the concentration of 16.6 wt. % loading.

The structure and texture of  $H_3PMo_{12}O_{40}$  (HPMo) and  $H_4PVMo_{11}O_{40}$  (HPVMO) supported on polyaniline was studied by XRD, FT-IR, low temperature nitrogen adsorption and scanning electron microscopy with EDS analysis. Thermal stability of both HPAs supported on polyaniline was studied by TG and DSC measurements.

Textural characteristics of the outgassed samples were obtained from nitrogen physisorption using a Micrometrics ASAP 2000 instrument. The specific surface area  $S_{BET}$ , mean cylindrical pore diameters  $d_p$  and adsorption pore volume  $V_{PN_2}$  were determined. Prior to the measurements the samples were degassed to  $10^{-5}$  Pa at  $150^\circ\text{C}$ . The BET specific surface area was calculated by using the standard Brunauer, Emmett and Teller method on the basis of the adsorption data. The pore size distributions were calculated applying the Barrett-Joyner-Halenda (BJH) method to the desorption branches of the isotherms. The IUPAC classification of pores and isotherms were used in this study.

Microstructure characterisation of the catalyst particles was carried out with a JEOL JSM 6460 LV instrument equipped with an OXFORD INSTRUMENTS EDS analyser. Powder materials were deposited on adhesive tape fixed to specimen tabs and then ion sputter coated with gold.

Powder X-ray diffraction data were obtained with a XD 8 Advanced Bruker diffractometer using the  $\text{Cu K}\alpha$  radiation in the range  $2\theta = 5-60^\circ$ .

The IR absorption spectra were recorded with a Jasco 430 spectrometer (spectral range  $4000-400\text{ cm}^{-1}$  range, 256 scans, and resolution  $2\text{ cm}^{-1}$ ) using KBr pellets.

Thermogravimetric analysis was performed on a Netzsch TG 209 derivatograph and on Netzsch DSC 204. The working conditions were as follows: samples amount 30-50mg for the supported samples; platinum crucible, heating rate 2.5K/min, 5K/min and 10K/min; nitrogen atmosphere.

### 3. Results and discussion

Characteristic parameters of the texture of PANI supported HPAs catalysts determined by BET measurements are summarized in Table 1.

Table 1. BET surface area and loading of PANI supported HPA prepared by impregnation method.

Sample	$S_{BET}$ , $\text{m}^2/\text{g}$	Pore volume, $V_{IP}$ , $\text{cm}^3/\text{g}$	Pore diameter, nm	HPA, wt %	Surface coverage, $\text{KU}/\text{nm}^2$
PANI	35.3	0.187	10.1	-	-
HPMo/PANI	37.7	0.111	2.20	16.6	2.1
HPVMO/PANI	36.9	0.140	2.23	16.6	2.2

The nitrogen adsorption isotherms of PANI and HPMo and HPVMO heteropolyacids supported on PANI respectively are shown in Figs. 1a, 2a and 3a. For both HPMo/PANI and HPVMO/PANI we observe a type II

isotherm with a type H3 hysteresis loop in the high range of relative pressure. For the values of relative pressure higher than 0.8 condensation take place giving a sharp adsorption volume increase. This behavior indicates that these samples have a mesoporous character. Hysteresis loop H3 type shows that HPA/PANI samples consists of aggregates of plate-like particles, which possess non-rigid slit-shaped pores, which was additionally confirmed by SEM analysis. Both HPMo and HPVMO heteropolyacids supported on PANI present the type II isotherm with a type H3 hysteresis loop.

The pore size distributions were calculated by Barret-Joyner-Halenda (BJH) method applied to the desorption branches of the isotherms. BJH method is further used to check and to complete the previous results. From the pore size distribution curve of PANI result a median pore width of 44.5 nm (Fig. 1b). Pores with sizes belonging to the entire range characteristic for mesoporosity (2-50 nm) and macroporosity ( $d > 50\text{ nm}$ ) appear for PANI support. The pore size distribution curves of HPMo and HPVMO supported on PANI show a median pore width of 34.4 nm and 41.2 nm respectively (Fig. 2b, 3b). Pores with sizes belonging to the entire range characteristic for mesoporosity (2-50 nm) and little macroporosity appear for HPAs supported on PANI. The pore size distribution curves of HPAs/PANI have many maximums, especially in the mesoporosity range, showing a nonuniformity of the porous structure.

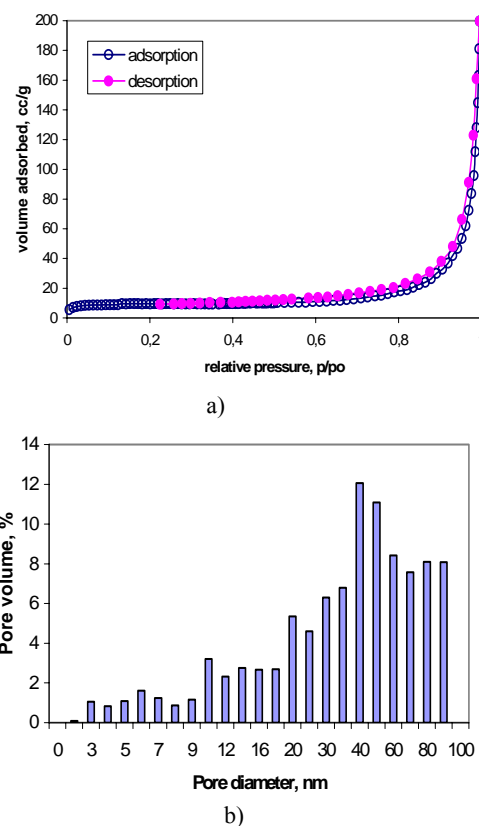
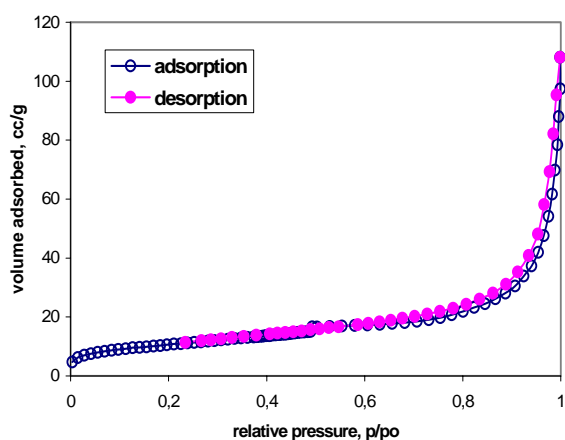


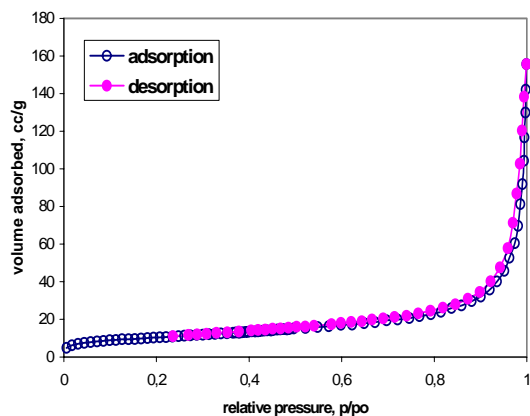
Fig. 1. Nitrogen adsorption-desorption isotherms at 77 K (a) and pore size distribution derived from the desorption branch of nitrogen physisorption (b) of PANI.

The specific surface area of PANI is  $35.3 \text{ m}^2/\text{g}$ , while the specific surface areas of HPAs deposited on PANI increased to  $37.7 \text{ m}^2/\text{g}$  for HPMo and to  $36.9 \text{ m}^2/\text{g}$  for HPVmo respectively (Table 1). The specific surface area of both HPAs supported on PANI increases slightly comparatively with the dedoped PANI, so the specific surface area could be assumed to be given by the support.

The mean pore diameter varies from  $44.5 \text{ nm}$  for PANI support to  $34.4 \text{ nm}$  and  $41.2 \text{ nm}$  for PANI supported HPM and HPVM respectively, as it results from the pores size distribution curves. The decreasing of pore diameter for PANI supported HPAs could be explain owing to support pores blocking by active phase, as well as by the formation of some HPAs crystallites agglomeration.

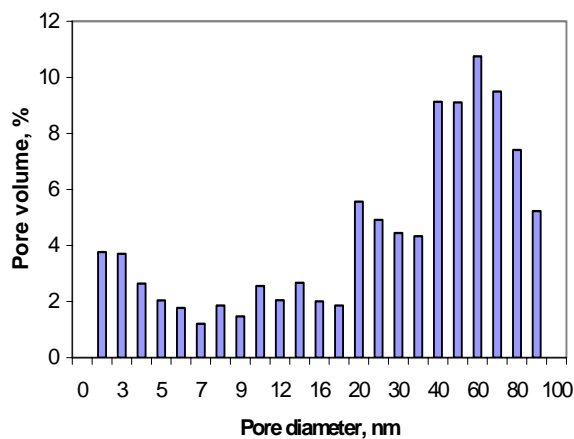


a)

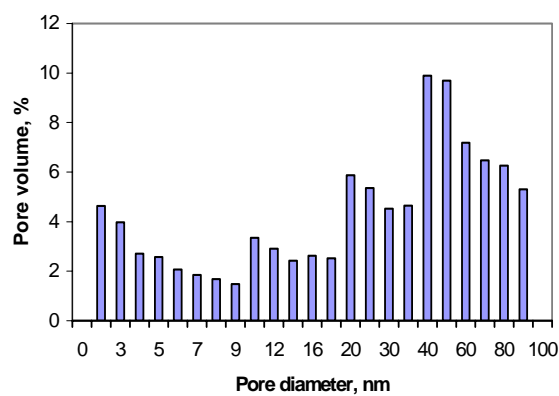


b)

Fig. 2. Nitrogen adsorption-desorption isotherms at  $77 \text{ K}$  (a) and pore size distribution derived from the desorption branch of nitrogen physisorption (b) of HPM supported on PANI



a)



b)

Fig. 3. Nitrogen adsorption-desorption isotherms at  $77 \text{ K}$  (a) and pore size distribution derived from the desorption branch of nitrogen physisorption (b) of HPVM supported on PANI

PANI support exhibit differential pore size distribution in the mesoporosity range and macroporosity range, while both PANI supported HPAs exhibit differential pore size distribution in the mesoporosity range and with only little macroporosity.

In order to confirm the presence of the Keggin anion on PANI, the supported HPAs samples were analysed by FTIR. The  $\text{PMo}_{12}\text{O}_{40}^{3-}$  Keggin ion structure consists of a  $\text{PO}_4$  tetrahedron surround by four  $\text{Mo}_3\text{O}_{13}$  formed by edge-sharing octahedra. These groups are connected each other by corner-sharing oxygen. This structure gives rise to four types of oxygen, being responsible for the fingerprints bands of Keggin ion between  $1200$  and  $700 \text{ cm}^{-1}$ . The specific absorption IR bands of PANI pure polymer are reported to occur at about  $1590$ ,  $1504$ ,  $1306$ ,  $1167$  and  $832 \text{ cm}^{-1}$  corresponding to C=C bonds of quinoid units, C=C bonds of benzenoid units, C-N stretching mode, N=Q=N stretching mode and C-H aromatic in-plane bending mode respectively [22].

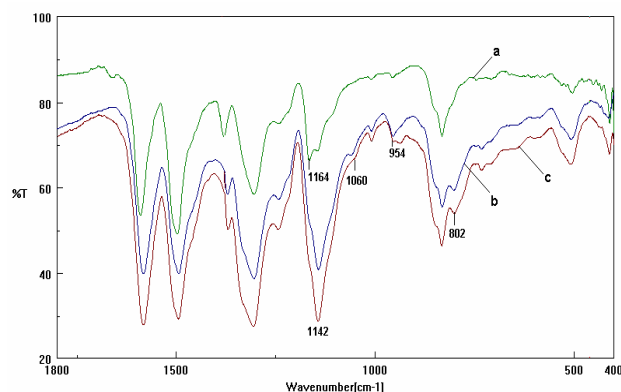


Fig. 4. FTIR spectra of a) polyaniline, b) polyaniline supported HPMo and c) polyaniline supported HPVMo Samples.

The pure HPAs show an IR spectrum with the specific absorption bands of the Keggin structure at  $1064\text{ cm}^{-1}$ ,  $965\text{ cm}^{-1}$ ,  $864\text{ cm}^{-1}$ ,  $805\text{ cm}^{-1}$  assigned to the stretching vibrations  $\nu_{\text{as}}\text{ P-O}$ ,  $\nu_{\text{as}}\text{ Mo=O}_t$ ,  $\nu_{\text{as}}\text{ Mo-O}_c\text{-Mo}$  and  $\nu_{\text{as}}\text{ Mo-O}_c\text{-Mo}$  respectively [31, 32].

These bands are preserved on the PANI supported samples, but they are broadened and partially obscured because of the strong absorption bands of PANI (Figure 4). The Keggin type characteristic IR bands of HPAs in PANI supported samples were observed at shifted positions by comparison with those of unsupported HPAs. In the IR spectra of PANI sample a strong band at  $1164\text{ cm}^{-1}$  is observed, this band being attributed to non-protonated base form [18]. In the IR spectra of PANI supported HPAs this band became weak (shoulder), but another strong band characteristic of the protonated states appeared at  $1142\text{ cm}^{-1}$  in both HPM and HPVMo catalysts.

Therefore the above results show that HPAs were supported on the PANI matrix as a charge-compensating components.

The replacing of a Mo atom with a V one leads to the appearance of two “shoulders” corresponding to the absorption maxim of the vibration  $\nu_{\text{as}}(\text{P-O}_p)$  at  $1080\text{ cm}^{-1}$  and  $\nu_{\text{as}}(\text{V-O}_T)$  at  $980\text{ cm}^{-1}$ . This confirms the presence of  $\text{V}^{5+}$  inside the  $\text{MO}_6$  octahedral. These shoulders could not be seen in the IR spectra of supported HPAs as adsorption bands of PANI overlap them completely.

The XRD patterns of PANI, unsupported HPM and PANI supported HPM are showed in Figure 5. As PANI support is an amorphous material it showed no characteristic XRD patterns. Also PANI supported HPM showed no characteristic XRD patterns probably because the active phase did not exist as a crystalline form but it was highly dispersed as fine particles on the PANI support matrix. M. Hasik et al [16] show that HPM was selectively immobilized on the cationic sites of PANI matrix in the HPM/PANI catalyst by quasi-ionic bond.

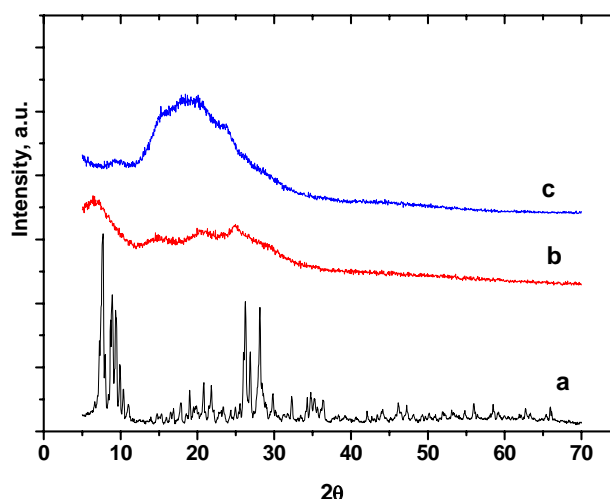


Fig. 5. XRD patterns of a)  $\text{H}_3\text{PMo}_{12}\text{O}_{40}$ ; b) HPMo/PANI; c) PANI.

The TG, DTG and DSC thermal curves of PANI and PANI supported HPAs are presented in Figure 6 a, b. Thermogravimetric curves TG and DTG of polyaniline show a decrease of mass (ca. 4%) within the temperature region  $50\text{--}100^\circ\text{C}$  and two endothermic DTG peaks at  $50$  and  $95^\circ\text{C}$ . The weight changes in this region is associated with release of solvents and water from the samples. After a further slight loss, the mass of the PANI sample became relatively constant in the temperature region  $200\text{--}360^\circ\text{C}$ . The DTG curve shows that the decomposition process of PANI backbone chains started at ca.  $400^\circ\text{C}$  and the minimum of endothermic DTG peak appear at  $510^\circ\text{C}$ .

The thermal curves of both HPAs supported on PANI did not show the effects characteristic of parent acids and resembled the thermal curve of pure PANI. The main decomposition processes of HPMo and HPVMo are: the hydrated water elimination, the decomposition of the anhydrous acids by constitutive water removal and finally the crystallisation process of Mo and V oxides [33-35]. The thermal curves of PANI and PANI supported HPAs exhibit only two processes, the hydrated water elimination in one or two steps and the decomposition of the polymer.

The decomposition of PANI supported HPAs take place at lower temperature than for PANI support (endothermic DTG peak at  $460^\circ\text{C}$  for HPVMo and at  $435^\circ\text{C}$  for HPMo). The same observation results from DSC curves examination. The DSC exothermic peaks corresponding to decomposition temperature of PANI supported HPAs are below the PANI support one (Fig. 6b).

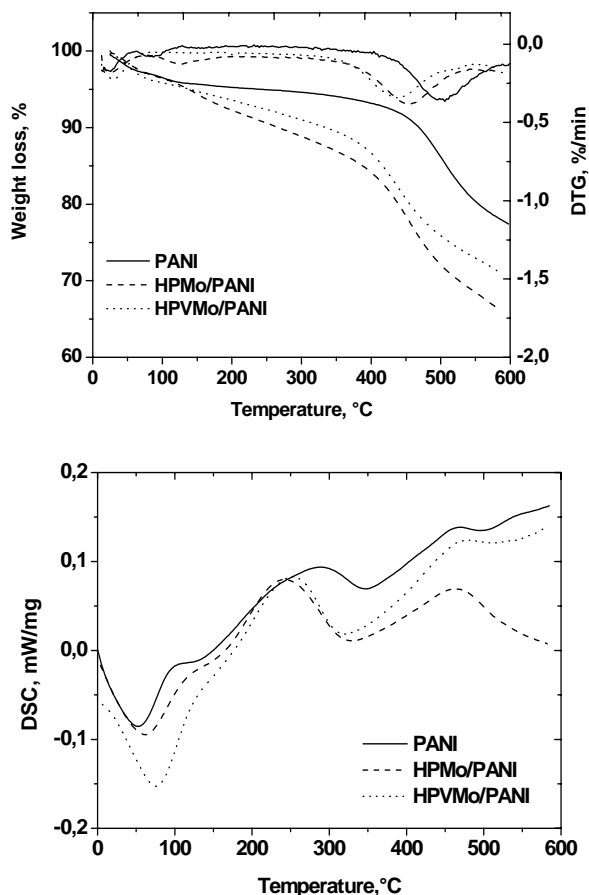


Fig. 6. Thermogravimetry analyses of PANI supported HPAs: a) TG-DTG and b) DSC analysis.

PANI support is composed of agglomerates of irregular shape particles with an average diameter below  $0.5 \mu\text{m}$  and a marked polydispersity in size (Figure 7). The surface morphology of PANI-supported HPAs is practically identical to that of the pure polymer (Figure 8). From SEM images one can see that no separate crystallites of the bulk phase of HPAs were found in the supported samples.

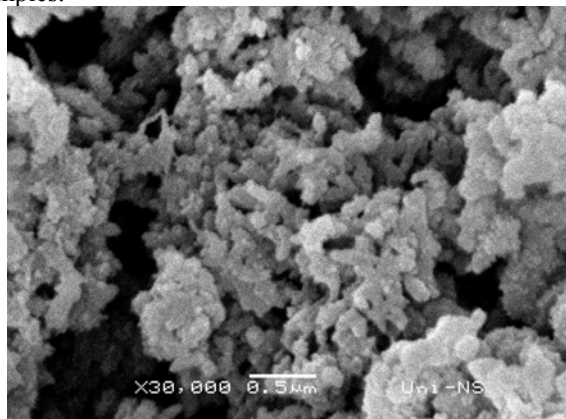


Fig. 7. SEM micrographs of PANI.

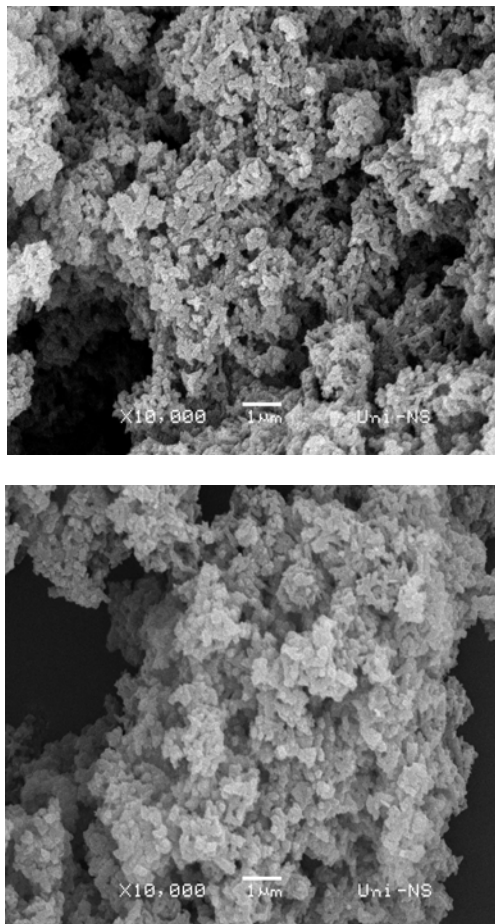


Fig. 8. SEM micrographs of HPM/PANI (a) and HPVMo/PANI (b)

HPAs distribution on supported samples surface was analysed by EDS method, which was performed as point analysis on thin particles. By this technique were obtained the chemical composition of carbon from PANI and Mo, V and P elements of heteropolyacid. The EDS point analysis was made over several domains with  $10 \times 10 \mu\text{m}$  dimensions on the same sample. The analysis was repeated on different samples in order to ensure the reproducibility of the obtained results.

Microanalytical data of EDS analysis show that the molybdenum and phosphorous (HPM/PANI) and molybdenum, phosphorous and vanadium (HPVM/PANI) content is homogeneous and close to stoichiometric values. In the case of PANI supported HPM the content of Mo as % wt. is 9.5 (stoichiometric value 10.4), while P content is 0.3 (stoichiometric value 0.28). For PANI supported HPVM the content of Mo as % wt. is 9.6 (stoichiometric value 10.7), P content is 0.3 (stoichiometric value 0.29) and V content is 0.42 (stoichiometric value 0.47) (Fig. 9 a, b).

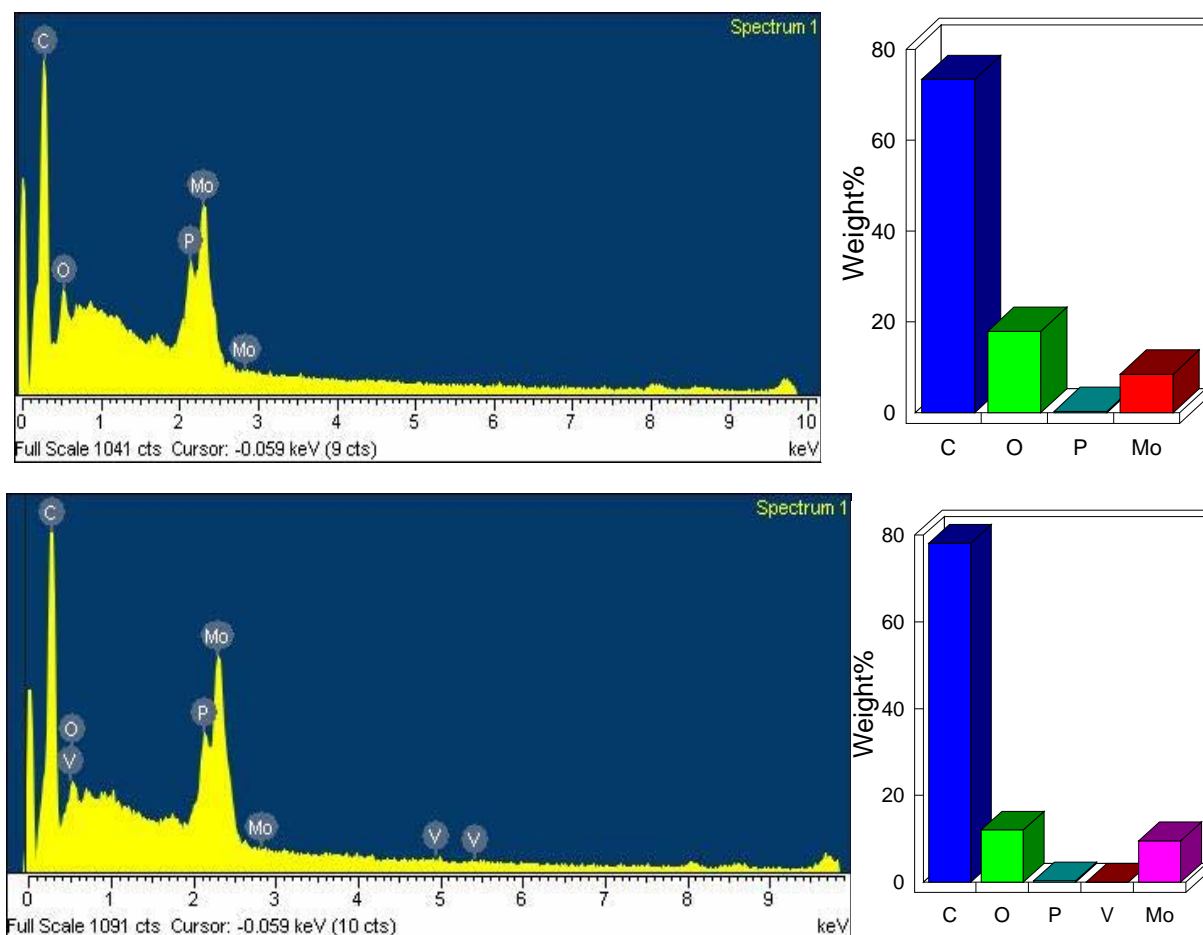


Fig. 9. a, b Microanalytical data of a  $10 \times 10 \mu\text{m}$  area and quantitative results of HPMo/PANI (a) and HPVMo/PANI (b)

#### 4. Conclusions

The thermal stability of PANI-supported heteropolyacids is given by thermal stability of the PANI support. The thermal decomposition of PANI support started at ca.  $400^\circ\text{C}$  and the minimum of endothermic DTG peak appear at  $510^\circ\text{C}$ , while for PANI supported HPAs a decrease of decomposition temperature are observed (endothermic DTG peak at  $435^\circ\text{C}$  for HPMo/PANI and  $460^\circ\text{C}$  for HPVMo/PANI).

FT-IR studies showed that HPAs anions preserved their Keggin structure after deposition on polyaniline support. X-ray diffraction and SEM studies confirmed the uniformity of the distribution of active phase in the bulk of the samples. By deposition on polyaniline, the values of specific surface area of both HPAs increased from 3-4  $\text{m}^2/\text{g}$  to 37.7  $\text{m}^2/\text{g}$  for HPMo/PANI and 36.9  $\text{m}^2/\text{g}$  for HPVMo/PANI, respectively.

Both PANI supported HPAs exhibit differential pore size distribution in the mesoporosity range and with only little macroporosity. The pore size distribution curves of HPAs/PANI have many maximums in the mesoporosity range, showing a nonuniformity of the porous structure.

It is found that most of active phases HPMo and HPVMo in samples are well dispersed on the support and

PANI-supported HPAs still keep its Keggin structure. The surface morphology of the PANI-supported samples is almost similar to that of PANI support, and thereby a relatively uniform distribution of active phase in the support pores is observed.

#### Acknowledgement

These investigations were partially financed by the Ministry of Education and Research of Romania Grant No 32826/2004 and Ministry of Science and Environment Protection of the Republic of Serbia – Project 1368.

#### References

- [1] F. Cavani, Catal. Today **41**, 73 (1998)
- [2] N. Mizuno, M. Misono, Chem. Rev. **98**, 199 (1998)
- [3] M. Misono, Catal. Rev. - Sci. Eng. **29**, 269 (1987)
- [4] E. Cadot, C. Marshal, M. Fournier, A. Teze, G. Herve, in Polyoxometalates, M.T. Pope and A. Muller (eds), Kluwer Acad. Publish., Dordrecht 1994, p.315.
- [5] Y. Ono in Perspectives in Catalysis, J.M. Thomas, K. I. Zamaraev (eds), London. 1992, p.341

- [6] S. Damyanova, J. L. G. Fierro, *Chem. Mater.* **10**(3), 871 (1998).
- [7] C. Trolliet, G. Coudurier, J.C. Vedrine, *Topics in Catal.* **15**(1), 73 (2001).
- [8] P. Vazquez, L. Pizzio, C. Caceres, M. Blanco, H. Thomas, E. Alesio, L. Finkielstein, B. Lantano, G. Moltrasio, J. Aguirre, *J. Mol. Catal. A-Chemical* **161**, 223 (2000).
- [9] I. V. Kozhevnikov, S. Holmes, M. R. H. Siddiqui, *Appl. Catal., A: General* **214**, 47 (2001).
- [10] F. -X. Liu-Cai, B. Sahut, E. Faydi, Aline Auroux, G. Herve, *Appl. Catal. A:General* **185**, 75 (1999).
- [11] J. Haber, K. Pamin, L. Matachowski, D. Mucha, *Appl. Catal. A: General*, **256**, 141 (2003).
- [12] A. Popa, V. Sasca, E. E. Kiss, Radmila Marinkovic-Neducin, M.T.Bokorov, J.Halasz, *J. Optoelectron. Adv. Mater.* **7**(6), 3169 (2005).
- [13] A. Popa, V. Sasca, M. Ștefănescu, E. E. Kis, R. Marinkovic-Neducin, *J.Serb.Chem.Soc.* **71**(3), 235 (2006)
- [14] A. Popa, V. Sasca, Radmila Marincovic-Neducin and Erne.E.Kis, *Rev. Roum.Chim.*, in press
- [15] M. Hasik, A. Pron, I. K. Bajer, J. Pozniczek, A. Bielanski, Z. Piwowska, R. Dziembaj, *Synthetic Metals* **55-57**, 972 (1993).
- [16] M. Hasik, J. Pozniczek, Z. Piwowska, R. Dziembaj, A. Bielanski, A.Pron, *J. Mol. Catal.* **89**, 329 (1994).
- [17] R. Dziembaj, A. Malecka, Z. Piwowska, A. Bielanski, *J. Mol. Catal. A: Chemical* **112**, 423 (1996).
- [18] S. S. Lim, G. I. Park, J. S. Choi, I. K. Song, W. Y. Lee, *Catal. Today* **74**, 299 (2002)
- [19] J. Pozniczek, I. K. Bajer, M. Zagorska, M. Hasik, A. Bielanski, A. Pron, in *Proc. 10<sup>th</sup> Int. Congr. Catal.*, Budapest, L.Gucz (Eds), Elsevier, Amsterdam 1993, p. 2593.
- [20] P. J. Kulesza, M. Chojak, K. Miecznikowski, A. Lewera, M. A. Malik, A. Kuhn, *Electrochem. Commun.* **4**, 510 (2002).
- [21] S.Palaniappan, M.S.Ram, *Green Chemistry* **4**, 53 (2002).
- [22] D. Han, Y. Chu, L. Yang, Y. Liu, Z. Lu, *Colloids and Surfaces A: Physicochem. Eng. Aspects* **259**, 179 (2005)
- [23] E. M. Genies, A. Boyle, M. Lapkowski, C. Tsintavis, *Synth. Met.* **36**, 139 (1990).
- [24] J. P. Travers, F. Genoud, C. Menardo, M. Nechtschein, *Synth. Met.* **35**, 159 (1990).
- [25] A. G. MacDiarmid, A. J. Epstein, *J. Chem. Soc., Faraday Discuss.* **88**, 317 (1989).
- [26] F. Lux, *Polymer* **35**, 2915 (1994).
- [27] B. Keita, K.Essaadi, J. P. Haeussler, *J. Electroanal. Chem.* **243**, 481 (1988).
- [28] G. Bidan, E. M. Genies, M. Lapowsky, *J. Electroanal.Chem.* **255**, 303 (1988).
- [29] G. A. Tsigdinos, *Inorg. Chem.* **7**, 437 (1968).
- [30] F. Kern, St. Reif, G. Emig, *Appl. Catal.* **150**, 143 (1997).
- [31] C. Rocchiccioli-Deltcheff, M. Fournier, R. Frank, R. Thouvent, *Inorg. Chem.* **22**, 207 (1983).
- [32] A. J. Bridgeman, *Chem.Phys.*, **287**, 55 (2003).
- [33] V. Sasca, M. Ștefănescu, A. Popa, *J. Therm. Anal. Cal.* **56**, 569 (1999).
- [34] V. Sasca, M. Ștefănescu, A. Popa, *J. Therm. Anal. Cal.* **72**, 311 (2003).
- [35] A. Popa, V. Sasca, S. Crisan, M. Ștefănescu, *Ann. West Univ. Timișoara, ser.Chem.* **9**(1), 85 (2000).

\*Corresponding author: sandu@acad-icht.tm.edu.ro